



ALMA MATER STUDIORUM
UNIVERSITÀ DI BOLOGNA

ARCHIVIO ISTITUZIONALE DELLA RICERCA

Alma Mater Studiorum Università di Bologna Archivio istituzionale della ricerca

Atmospheric plasma assisted PLA/microfibrillated cellulose (MFC) multilayer biocomposite for sustainable barrier application

This is the final peer-reviewed author's accepted manuscript (postprint) of the following publication:

Published Version:

Atmospheric plasma assisted PLA/microfibrillated cellulose (MFC) multilayer biocomposite for sustainable barrier application / Meriçer, Çağlar; Minelli, Matteo; De Angelis, Maria G.; Giacinti Baschetti, Marco; Stancampiano, Augusto; Laurita, Romolo; Gherardi, Matteo; Colombo, Vittorio; Trifol, Jon; Szabo, Peter; Lindström, Tom. - In: INDUSTRIAL CROPS AND PRODUCTS. - ISSN 0926-6690. - ELETTRONICO. - 93:(2016), pp. 235-243. [10.1016/j.indcrop.2016.03.020]

Availability:

This version is available at: <https://hdl.handle.net/11585/567619> since: 2016-11-15

Published:

DOI: <http://doi.org/10.1016/j.indcrop.2016.03.020>

Terms of use:

Some rights reserved. The terms and conditions for the reuse of this version of the manuscript are specified in the publishing policy. For all terms of use and more information see the publisher's website.

This item was downloaded from IRIS Università di Bologna (<https://cris.unibo.it/>).
When citing, please refer to the published version.

(Article begins on next page)

This is the final peer-reviewed accepted manuscript of:

Çağlar Meriçer, Matteo Minelli, Maria G. De Angelis, Marco Giacinti Baschetti, Augusto Stancampiano, Romolo Laurita, Matteo Gherardi, Vittorio Colombo, Jon Trifol, Peter Szabo, Tom Lindström

Atmospheric plasma assisted PLA/microfibrillated cellulose (MFC) multilayer biocomposite for sustainable barrier application

In "Industrial Crops and Products" Volume 93, 2016, p. 235-243

The final published version is available online at:

<https://doi.org/10.1016/j.indcrop.2016.03.020>

Rights / License:

The terms and conditions for the reuse of this version of the manuscript are specified in the publishing policy. For all terms of use and more information see the publisher's website.

This item was downloaded from IRIS Università di Bologna (<https://cris.unibo.it/>)

When citing, please refer to the published version.

1 **Atmospheric plasma assisted PLA/Microfibrillated cellulose (MFC) multilayer**
2 **biocomposite for sustainable barrier application**

3 *Çağlar Meriçer,¹ Matteo Minelli,^{1,2} Maria G. De Angelis,^{1,2} Marco Giacinti Baschetti,^{*1,2}*
4 *Augusto Stancampiano², Romolo Laurita,^{2,3} Matteo Gherardi,^{2,3} Vittorio Colombo,^{2,3} Jon Trifol,⁴*
5 *Peter Szabo,⁴ Tom Lindström⁵*

6
7 ¹ DICAM – Dipartimento di Ingegneria Civile, Chimica, Ambientale e dei Materiali, Alma Mater
8 Studiorum –University of Bologna, Italy

9 ² CIRI-MAM – Centro Interdipartimentale per la Ricerca Industriale, Meccanica Avanzata e
10 Materiali, Alma Mater Studiorum –University of Bologna, Italy

11 ³ DIN – Dipartimento di Ingegneria Industriale, Alma Mater Studiorum –University of Bologna

12 ⁴ Danish Polymer Centre, Department of Chemical and Biochemical Engineering, Technical
13 University of Denmark, Denmark

14 ⁵ Innventia AB, Stockholm, Sweden

15

16

17 Corresponding author

18 Marco Giacinti Baschetti

19 Tel. +39 51 2090408

20 Fax. +39 51 6347788

21 e-mail: marco.giacinti@unibo.it

22

23 Highlights:

24 • MFC/PLA bilayer films are fabricated as biorenewable barrier solution for packaging.

25 • Atmospheric plasma activation guarantees the effectiveness of coating process.

26 • MFC coatings improve significantly the mechanical and barrier performances of PLA.

27 **ABSTRACT**

28 Fully bio-based and biodegradable materials, such as polylactic acid (PLA) and microfibrillated
29 cellulose (MFC), are considered in order to produce a completely renewable packaging solution
30 for oxygen barrier applications, even at medium-high relative humidity (R.H.). Thin layers of
31 MFC were coated on different PLA substrates by activating film surface with an atmospheric
32 plasma treatment, leading to the fabrication of robust and transparent multilayer composite films,
33 which were then characterized by different experimental techniques. UV transmission
34 measurements confirmed the transparency of multilayer films (60% of UV transmission rate),
35 while SEM micrographs showed the presence of a continuous, dense and defect free layer of
36 MFC on PLA surface. Concerning the mechanical behavior of the samples, tensile tests revealed
37 that the multilayer films significantly improved the stress at break value of neat PLA. Moreover,
38 the oxygen barrier properties of the multilayer films were improved more than one order of
39 magnitude compared to neat PLA film at 35°C and 0% R.H. and the permeability values are
40 maintained up to 60% R.H.. The obtained materials therefore showed interesting properties for
41 their possible use in barrier packaging applications as fully biodegradable solution, coupling two
42 primarily incompatible matrices in a multilayer film with no need of any solvent or chemical.

43

44 **Keywords:**

45 Nanocellulose, polylactic acid, atmospheric plasma, multilayer film, barrier properties

46

47

48

49 **1. INTRODUCTION**

50 Plastics derived from fossil fuels have been the commodity materials in the packaging industry
51 during last few decades and this trend has been increasing steadily mainly due to their feasibility
52 in terms of cost and manufacturing processes.(Plastics Europe, 2015) On the other hand, limited
53 recycling rates and waste-disposal problems associated with traditional plastic materials led to
54 serious environmental issues. (Mohanty et al., 2002). The latest data show that the packaging
55 industry accounts for nearly 40% of plastics usage in the world (Plastics Europe, 2015). Hence,
56 due to increasing environmental concerns and end-of-life cycles of commodity packaging
57 materials, over the last decade the research in developing eco-friendly and biodegradable
58 polymer solutions has reached its peak in packaging and other sectors. (Petersen et al., 1999; van
59 Tuil et al., 2000; Siracusa et al., 2008)

60 Bio-based materials can be divided into three main groups, according to the classification
61 based on their source: polymers derived directly from natural materials (starch, cellulose,
62 chitosan), synthesized from bio-derived monomers (polylactide - PLA, bio-polyethylene - PE
63 etc.) and produced by living organisms such as microorganisms or bacteria (poly hydroxyl
64 alkanoates - PHAs, bacterial cellulose) (Tharanathan, 2003; Klemm et al., 2006; Siró and
65 Plackett, 2010; Vieira et al., 2011; Johansson et al., 2012).

66 Among the different biomaterials, polylactide or polylactic acid (PLA) is a biodegradable
67 bioplastic produced by the polymerization reaction of a naturally derived monomer (lactic acid),
68 obtained from dextrose. Being renewable and biodegradable, it decomposes in the environment
69 into carbon dioxide and water in the appropriate conditions, PLA is a suitable candidate for the
70 replacement of petroleum based products (Jamshidian et al., 2010), and currently offers a strong
71 alternative in the packaging industry, also due to its easy processability through conventional

72 methods such as melt processing (Drumright et al., 2000; Nakagaito et al., 2009). For these
73 reasons, PLA has been already applied in the industry for certain food products or goods, and is
74 currently widely investigated aiming at the improvement of some key properties such as
75 physical, mechanical and gas barrier properties in order to better compete with oil derived
76 plastics (Auras et al., 2003, 2006; de Azeredo, 2009; Drieskens et al., 2009; Svagan et al., 2012;
77 Guinault et al., 2012; Delpouve et al., 2012; Bai et al., 2014). In particular, the gas barrier ability
78 still needs to be enhanced in order to use PLA in barrier packaging applications, e.g. for sensitive
79 foods (Auras et al., 2006; de Azeredo, 2009; Drieskens et al., 2009). In this concern, several
80 studies investigated the gas permeability of PLA-based materials, with particular attention to
81 nanocomposites, prepared following different approaches such as melt extrusion, in situ
82 polymerization, and solvent casting, to mix the polymer with impermeable layered silicate clays
83 (Chang et al., 2003; Chowdhury, 2008; Picard et al., 2011; Svagan et al., 2012). However, due
84 to difficult exfoliation and orientation of nanoclays, the reduction in oxygen permeability is
85 somewhat limited around 60% (Chang et al., 2003; Chowdhury, 2008).

86 Recently, the development of nanometric sized cellulosic materials, known as
87 microfibrillated cellulose (MFC or NFC) (Herrick et al., 1983; Turbak et al., 1983; Klemm et al.,
88 2006; Siró and Plackett, 2010) and nanowhiskers or nanocrystals, (Samir et al., 2005; Eichhorn,
89 2011) produced respectively by delamination of the fibers in a high pressure homogenization
90 process, and by acid hydrolysis to eliminate the amorphous regions of the fibrils, opened up new
91 possibilities for barrier packaging applications primarily due to the remarkable mechanical and
92 barrier properties of these new materials (Berglund, 2005; Samir et al., 2005; Fukuzumi et al.,
93 2009; Henriksson et al., 2008; Syverud and Stenius, 2009; Sanchez-Garcia and Lagaron, 2010;
94 Lavoine et al., 2012; Belbekhouche et al., 2011).

95 Strong and stiff films of nanocellulose can be produced from highly diluted dispersion in
96 water by different methods (Yano, and Nakahara, 2004; Syverud and Stenius, 2009; Minelli et
97 al., 2010; Österberg et al., 2013), and MFC can also be used as reinforcement for
98 nanocomposites to improve the mechanical properties due to high aspect ratio of the microfibrils
99 (Zimmermann et al., 2004; Leitner et al., 2007; Svagan et al., 2007; Iwatake et al., 2008).
100 Moreover, cellulosic materials can be easily functionalized thanks to the high number of
101 hydroxyl groups on the surface of microfibrils which create sites for chemical modifications
102 suitable to various applications (Andresen et al. 2007; Lu et al., 2008; Stenstad et al., 2008;
103 Siquera et al., 2009, Lavoine et al., 2014, Habibi, 2014).

104 MFC is a strong candidate for the fabrication of nanocomposites and coating formulations
105 for barrier packaging applications in view of its high crystalline content and the ability to form
106 dense interfibrillar network with hydrogen bonds, which eventually lead to excellent gas barrier
107 properties (Lavoine et al., 2012; Martínez-Sanz et al., 2013; Bardet et al., 2015, Rodionova et al.,
108 2012). The oxygen permeability of 21 μm thick MFC films produced from bleached spruce
109 sulfite pulp at 23 °C and 0% RH was reported as $1.9 \cdot 10^{-18}$ mol m/m² s Pa (Syverud and Stenius,
110 2009), comparable with well-known ultra-barrier polymers, e.g. polyvinyl alcohol, PVOH or
111 polyvinylidene chloride, PVdC (Lange and Wyser, 2003). The effect of pretreatments of the
112 cellulose fiber on the final MFC barrier performances has been also investigated, revealing that
113 O₂ permeability in enzymatically pretreated MFC is comparable if not slightly smaller than that
114 in carboxymethylated MFC, being the values measured at 35°C as low as $2.6 \cdot 10^{-19}$ and $6.3 \cdot 10^{-19}$
115 mol m/m² s Pa, for the two materials respectively (Minelli et al. 2010).

116 PLA and MFC are very likely the two most promising bio-based materials for industrial
117 application in the near future, and for this reason they were often combined to form new

118 generation of nanocomposites for different purposes (Iwatake et al., 2008; Suryanegara et al.,
119 2009; Mathew et al., 2005, 2006; Oksman et al., 2006; Iwatake et al. 2008). Interestingly, highly
120 loaded nanocomposite films (up to 90 wt.% of MFC) have been obtained from an aqueous
121 suspension of MFC and PLA followed by hot pressing of the dried sheets, leading to a tensile
122 modulus that increases linearly with the MFC content, followed by strength and strain at fracture
123 (Nakagaito et al. 2009). Alternatively, Fukuzumi et al. (2009, 2013) used a different approach
124 and prepared TEMPO oxidized MFC thin coating (0.4 μm) on plasma-treated PLA film, leading
125 to a dramatic reduction of the oxygen transfer rate. Plasma treatment can indeed modify the
126 surface properties of PLA films, such as wettability, surface energy and chemical structure
127 (Vergne et al., 2011; Jordá-Vilaplana et al., 2014; Cools et al., 2015), enabling and the deposition
128 of thin coatings on the polymer surface and the consequent production of multilayer films
129 (Benetto et al., 2015).

130 Although significant efforts have been devoted to the fabrication of PLA/nanocellulose
131 composite systems by dispersion of fibrils or crystals into the polymer matrix, very few works
132 have focused on their assembly in layered structures, which in turn are clearly more industrially
133 attractive, especially for packaging applications. The main limitation is indeed in the large
134 incompatibility of the two phases, which can be overcome by chemical modification, surface
135 treatments (Fukuzumi et al. 2009), or by means of specific deposition techniques (Aulin et al.
136 2013).

137 In the present study, a bilayer system is fabricated by coating a thin layer of MFC onto a
138 plasma activated PLA substrate, obtaining a strong adhesion between two primarily incompatible
139 layers. Mechanical, optical and transport properties of the multilayer films were analyzed with

140 particular attention to the oxygen barrier, which was investigated in both dry and humid
141 conditions, and compared with data for neat PLA and other current polymer commodities..

142

143 **2. Experimental**

144 *2.1. Materials*

145 *Microfibrillated cellulose (MFC)*

146 The neat MFC films and the coatings prepared in this work are obtained from aqueous
147 dispersions at about 2% by weight of solid contents, produced at Innventia AB (Stockholm,
148 Sweden). Two different MFC dispersions were used, often labeled as MFC generation 1 (MFC
149 G1) and MFC generation 2 (MFC G2), produced from cellulose pulp after identical mechanical
150 crushing in the high pressure homogenization step following different pretreatment procedures to
151 obtain an easier and energy efficient fibrillation process. In particular, MFC G1 is obtained by an
152 enzymatic pretreatment of the cellulose pulp, as described by Pääkkö et al. (2007), a
153 carboxymethylation process is used to fabricate MFC-G2, according to Wågberg et al. (2008). A
154 brief description of the preparation techniques of the MFC productions is here proposed, while
155 more detailed illustration of the method and the results of their physical and morphological
156 characterization are in the cited publications (Henriksson et al., 2007; Siró et al., 2011); .

157 MFC G1 is produced from commercial bleached sulfite softwood pulp (Domsjö ECO
158 Bright, Domsjö Fabriker AB, Sweden) consisting of 40% pine (*Pinus sylvestris*) and 60% spruce
159 (*Picea abies*) with a hemicellulose content of 13.8% and a lignin content of 1%, whereas
160 commercial sulfite softwood dissolving pulp (Domsjö Dissolving Plus, Domsjö Fabriker AB,
161 Sweden), with 4.5% of hemicellulose and 0.6% of lignin content, has been used to obtain the
162 final MFC G2 dispersion.

163 The fabrication of the pure MFC films is carried out by further diluting the dispersions
164 with deionized water in order to prepare a suspension that could be easily poured (1% of solid
165 content for MFC G1, and 0.67 for MFC G2), which is then vigorously stirred for about 3 h and
166 finally cast in glass Petri dishes placed under a clean hood at room temperature, until complete
167 solvent evaporation is attained.

168 *Poly(lactic acid) (PLA)*

169 Two different types of PLA are used as substrate, in order to explore any possible
170 difference in the plasma activation process and in the final barrier properties; to this aim
171 amorphous (PLA-Am) and semi-crystalline PLA are accounted for.

172 Amorphous PLA films were produced by solvent casting, dissolving Natureworks (4060D)
173 pellets in dichloromethane 5% wt., vigorously stirring the solution for about 3 h, and finally
174 pouring it into glass Petri dish which was then placed in a clean hood at ambient conditions for
175 24 h, until the solvent was completely evaporated. The films obtained were then treated under
176 vacuum at 50°C to ensure the complete solvent evaporation.

177 Semi-crystalline PLA (Polybio 212) was a commercially available product obtained by
178 extrusion, and kindly provided by Coopbox S.p.A; the film has a thickness of 40 µm, a
179 crystalline fraction of about 18%, as obtained by DSC measurements.

180

181 *2.2. Atmospheric Plasma treatment*

182 PLA films were plasma treated by means of two different Dielectric Barrier Discharge (DBD)
183 sources, named planar-DBD and DBD-roller; during the treatment, PLA films were positioned in
184 the interelectrode gap on the grounded electrode of the DBD plasma sources.

185 The DBD-roller, whose details have been previously illustrated, (Boselli et al. 2012), was
186 specifically designed to enable a roll-to-roll continuous treatment of films. The plasma source
187 was operated in air driven by a high voltage generator (FID GmbH – FPG 20–1NMK), and the
188 treatment was performed using peak voltage (PV) of 20 kV and pulse repetition frequency (PRF)
189 of 330 Hz and was operated for 20 s. A planar-DBD source, also described in a previous work
190 (Boselli et al. 2013), was operated in air as well, driven by a high voltage generator (Trek model
191 30/20-H-CE), connected to a function generator (Stanford Research model DS335). The
192 operating parameter of the high voltage generator were set as follows: bipolar square-wave
193 having a PV of 12.7 kV and a PRF of 100 Hz. PLA films were treated for 5 minutes.
194 No bulky effect is expected to be produced by the plasma process, which is ultimately an almost
195 purely superficial treatment: its penetration is indeed in the order of few hundreds of nanometers,
196 not able to produce significant changes in the overall properties of the PLA film. In this respect,
197 the gas transport properties of PLA films have been demonstrated to be practically unchanged by
198 the plasma treatment (Boselli et al., 2013).

199

200 *2.3 multilayer film preparation*

201 PLA/MFC films are prepared by solvent casting of the MFC dispersion on top of a plasma
202 treated PLA film conveniently located in a glassy Petri dish; alternatively adjustable casting
203 knife technique was used on rectangular glass support (BYK-Gardner). Multilayer films are then
204 obtained after the evaporation of water in a clean hood at ambient conditions for 2-3 days. The
205 thicknesses of the films used in the different tests span from 10 to 60 microns (Table 1). They
206 were obtained by controlling the exact amount of solution poured in the petri dish during casting
207 procedure. The resulting thicknesses were then measured with a Mitutoyo micrometer (Mitutoyo

208 Scandinavia AB, Väsby, Sweden) in 10 different spots, resulting deviation, on the single sample,
209 not exceeding 5 %.

210 It is noteworthy that the bilayer systems are obtained only after the plasma treatment of the
211 PLA film surface. In absence of any activation, indeed, no adhesion at all could be achieved
212 between coating and substrate.

213

214 **Table 1.** Bilayer films characterized in this study with their thicknesses and analyzing methods.

Film	Thickness range (μm)
PLA	40
PLA-Am	40-50
MFC G1	9-32
MFC G2	10-27
PLA/MFC G1	40 + 10-17
PLA/MFC G2	40 + 7-17

215

216 *2.4. Material characterization*

217 *Scanning electron microscope (SEM)*

218 The materials were characterized by SEM on an FEI Quanta 200 ESEM FEG at 5 kV.
219 SEM images were obtained in order to investigate the arrangement of the different layers in the
220 bilayer structure. Indeed, MFC G1 and MFC G2 coatings on top of PLA substrates were
221 expected to show a dense and continuous layer, as typically observed for self-standing
222 nanocellulose films (Minelli et al. 2010).

223 *Tensile tests*

224 Tensile tests were carried out by means of an INSTRON 4301 apparatus (Instron
225 Engineering Corporation, Canton, MA, USA) at a strain rate of 1 mm min^{-1} for PLA-Am, MFC

226 G2 and PLA/MFC G2 films, in order to inspect the stability of the coating application and to
227 ensure that the adhesion between two layers is retained as well as the mechanical properties are
228 preserved. Wide rectangular shaped specimens with a dimension of 50x10 mm were prepared for
229 testing. The Young modulus was determined from the slope of the linear region of the stress-
230 strain range (approximately between 1% and 6% of strain).

231 *Optical properties*

232 UV light transmissions of PLA-Am, MFC G1, MFC G2, PLA/MFC G1 and PLA/MFC G2
233 films were measured using a UV-Vis spectrometer (Polar Star Omega) in the range of 220 nm –
234 1000 nm by triplicate.

235 *Gas permeation apparatus*

236 Gas permeation experiments were carried out in two different apparatuses, namely dry and
237 humid permeation systems, already described in previous studies (Minelli et al. 2008, 2010).
238 Both pieces of equipment exploit a standard barometric technique for the evaluation of the
239 permeate flux from the measure of a pressure increase in a closed downstream compartment,
240 whose volume has been previously calibrated (ASTM Standard D 1434). Humid gas tests were
241 carried out conveniently pre-equilibrating the sample at the desired humidity by exposing both
242 sides of the film to pure water vapor at controlled pressure (corresponding to the target activity).
243 Therefore, when one side of the sample is fed by a humidified O₂ stream at the same RH of the
244 preequilibration step, the water has the same chemical potential in both upstream and
245 downstream compartment and only oxygen permeates through (Minelli et al., 2008; Ansaloni et
246 al., 2014). Thus, at steady state conditions Eq. 1 provides the required expression for
247 permeability:

248
$$P = O.T.R. \cdot \delta = \left(\frac{dp}{dt} \right)_{t \rightarrow \infty} \cdot \frac{V}{R \cdot T \cdot A} \cdot \frac{\delta}{\Delta p} \quad (1)$$

249 being V the downstream volume (23 cm³), A the permeation area (9.6 cm²), δ the sample
250 thickness, and Δp the pressure difference across the film (about 1 bar), whereas O.T.R. is the
251 oxygen transmission rate. The uncertainty in the permeation measurement can be estimated
252 within $\pm 10\%$ of the reported values.

253

254 **3. Results and discussion**

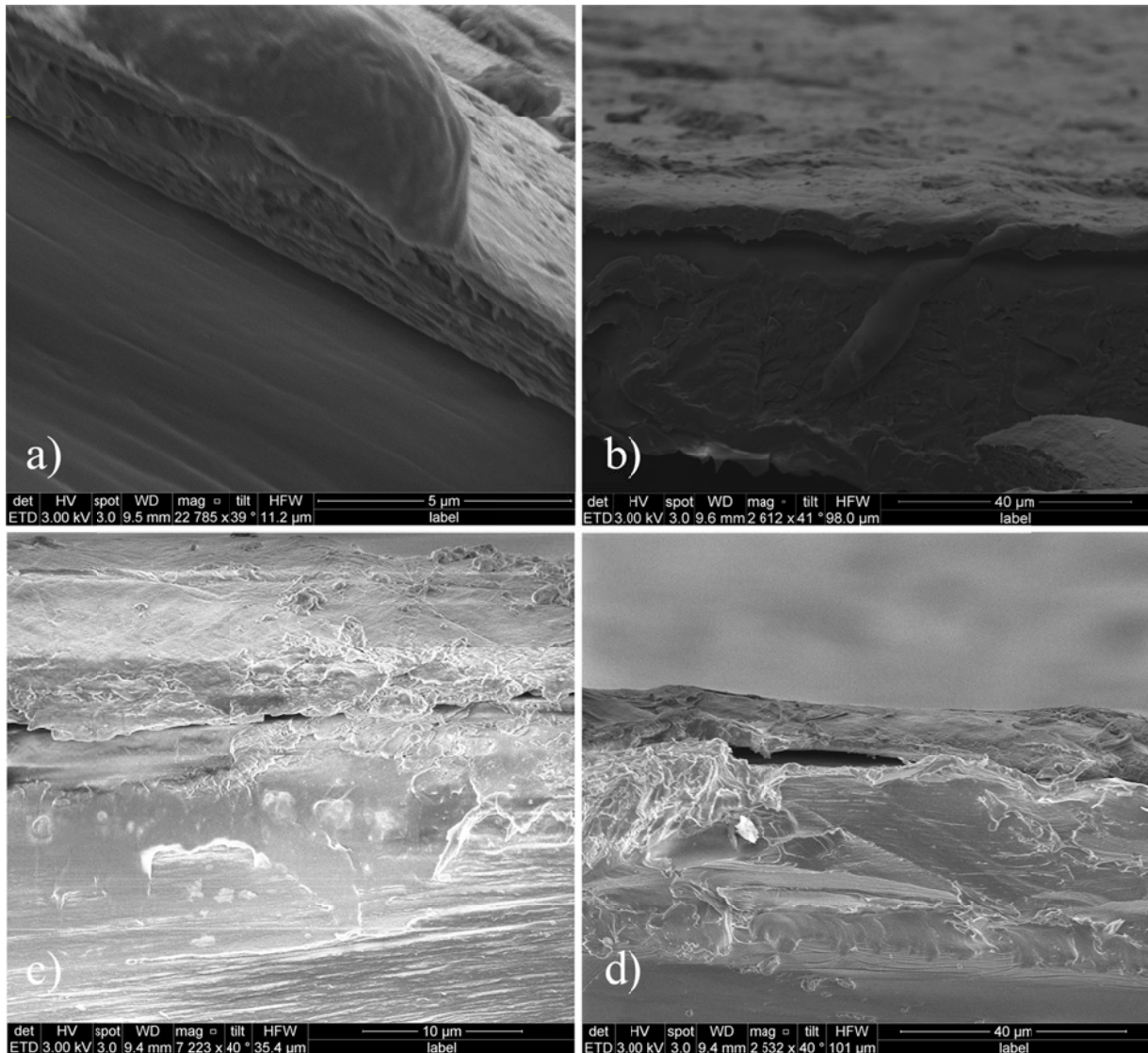
255 PLA/MFC multilayer films obtained after plasma treatment are robust, stable and resistant
256 even after the successive cycles of permeability tests at various relative humidity conditions.
257 Indeed a remarkable adhesion is achieved between the two layers, and the coating cannot be
258 peeled off even after bending or stretching the multilayer samples in atmospheric air; the sample
259 is also able to resist to exposure to saturated water environment before each permeation test in
260 the conditioning step. Interestingly, no aging effect has been observed; the two layers of the
261 MFC/PLA samples, stored in standard room conditions of temperature and relative humidity, are
262 still well attached after in almost one year after their preparation.

263 The effective adhesion is obtained for MFC types produced both with enzymatic
264 pretreatment (G1) and carboxymethylation pretreatment (G2), and on top of all PLA substrates
265 investigated (semicrystalline or amorphous polylactide). The multilayer films were then tested in
266 order to investigate the structural stability and their performances, and the results are presented
267 in the following sections.

268

269 *3.1. SEM images*

270 SEM micrographs of the cross section of PLA/MFC G1 and PLA/MFC G2 multilayer
271 films are shown in Fig. 1a-d below, with two different magnifications for each sample. A dense
272 and continuous layer of MFC coating is clearly visible in all figures, similarly to the SEM
273 micrographs already reported for self-standing MFC films (Minelli et al. 2010); the apparent
274 thickness obtained from the images is in the range of 3-10 and 4-13 μm for MFC G1 and G2,
275 respectively, thus only slightly lower than the values measured by the digital micrometer. Small
276 defects around the edges of the samples can be attributed to the cutting procedure, performed
277 after freezing the sample in liquid nitrogen, which was required for cross section SEM analysis.



278

279

Fig. 1. SEM micrographs of PLA/MFC G1 (a, b) and PLA/MFC G2 films (c, d)

280

281 *3.2. Mechanical properties*

282

283

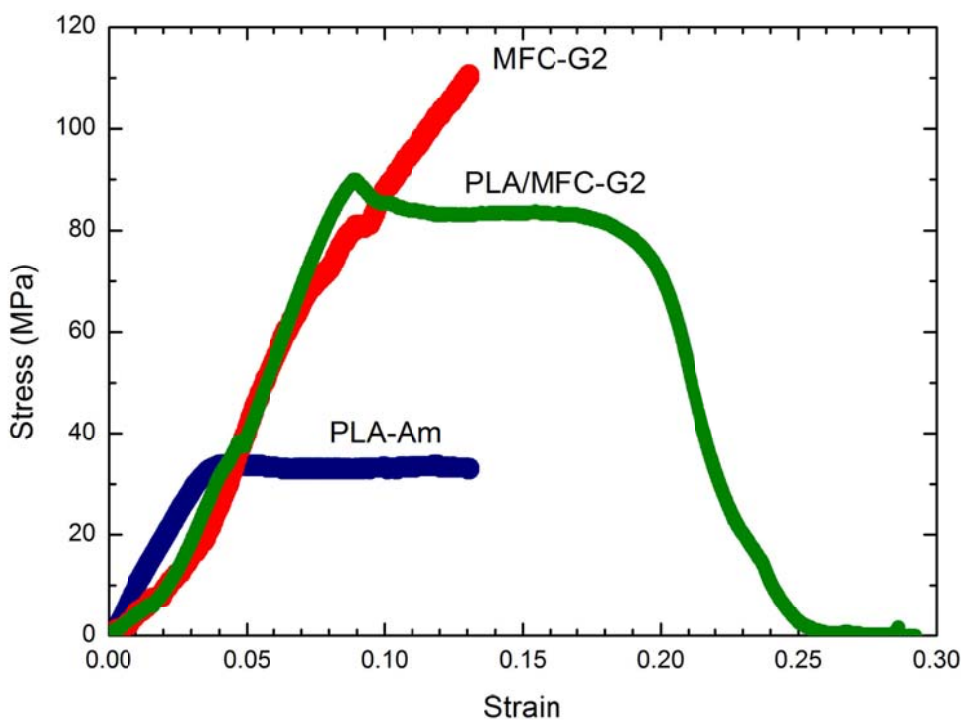
284

285

The tensile tests carried out on PLA-Am, MFC G2 and PLA/MFC G2 multilayer films provided the values of strain at break, stress at break and Young modulus, which are reported in Table 2, while the stress-strain curves are illustrated in Fig. 2. Interestingly, the results show that the MFC coating improved appreciably the Young modulus and stress at break values of neat

286 PLA, reaching the characteristic values of neat MFC, with no failure of the bilayer system. The
 287 values of stress at break and Young's modulus obtained for pure PLA are lower than the usual
 288 literature values, likely in view of some experimental error produced by the absence of an
 289 extensometer, although the observed behavior is the same reported from other authors(see e.g.
 290 Renouf-Glauser et al., 2005).

291



292

293 **Fig. 2.** Stress-strain curves for amorphous PLA-Am, self-standing MFC-G2 film, and PLA/MFC
 294 G2 bilayer film

295

296 **Table 2.** Mechanical properties of the films investigated in this study.

Film	Stress at break (MPa)	Strain at break (%)	Young's modulus (GPa)
PLA-Am	36 ± 4	19 ± 7	0.7 ± 0.2

MFC G2	94 ± 16	10 ± 3	1.0 ± 0.1
PLA/MFC G2	86 ± 1	-	1.12 ± 0.01

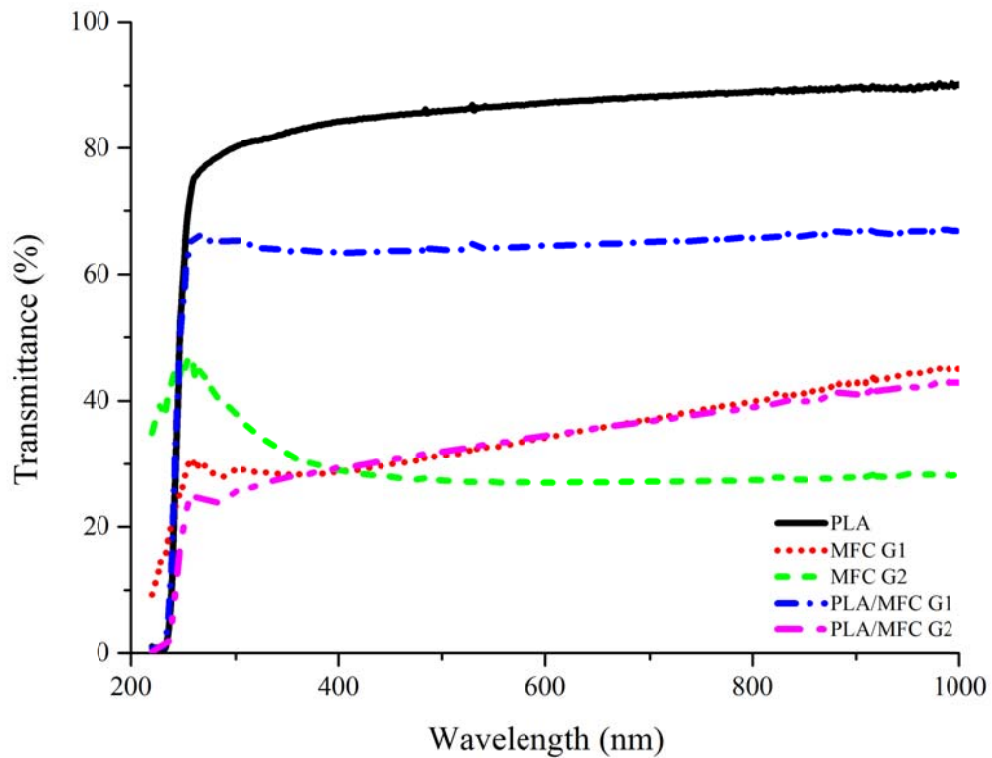
297

298 The results from mechanical tests confirmed the strong adhesion between PLA substrate
299 and the dense MFC layer, which was able to prevent any delamination before the ultimate stress
300 of the single MFC layer is reached. The mechanical properties of MFC G2 are comparable with
301 those reported in a previous study (Plackett et al. 2010) for the same material except Young's
302 modulus, which is lower in this study likely due to different casting procedures, which produced
303 different packing of nanofiber networks. The testing procedure and setup, as well as the
304 preparation protocol of MFC films are indeed the main causes of the literature data variability,
305 which affect MFC mechanical properties (Svagan et al., 2007; Henriksson and Berglund, 2007;
306 Henriksson et al., 2008).

307

308 *3.3. Optical properties*

309 Fig. 3 illustrates the UV transmittance spectra of PLA, MFC G1, MFC G2, PLA/MFC G1
310 and PLA/MFC G2 films, revealing that the transmittance at 600 nm (center of visible light
311 spectrum) is about 87, 34, 27, 64 and 34%, respectively. PLA is practically transparent (almost
312 90% of transmittance), while MFC is typically opaque, and its effect on the overall behavior is
313 clearly apparent. As one can see, the difference in the opacity of the two types of MFC (in the
314 self standing films) is definitely not significant, as also reported in a previous work (Plackett et
315 al., 2010). It is noteworthy, however, that PLA/MFC G1 sample showed satisfying transparency
316 of 64% compared to PLA/MFC G2, even though its MFC layer was slightly thicker (about 17
317 μm for MFC G1 coating, and about 10 μm for the MFC G2 one).



318
 319 **Fig. 3.** UV light transmission of the films investigated in this study
 320

321 *3.4. Barrier properties*

322 The dry oxygen permeability of PLA, PLA-Am, MFC G2 and PLA/MFC G2 films was
 323 measured in the dry permeation apparatus in temperature range of 25-45 °C, and the results are
 324 illustrated in Fig. 4. Results confirm that the increased crystallinity improves the barrier
 325 properties of PLA as the amorphous PLA has higher oxygen permeability compared to semi-
 326 crystalline PLA used in this study (18% crystallinity). Same measurements were carried out for
 327 neat MFC G2 and PLA/MFC G2 films in the same temperature range, and the improvement in
 328 oxygen barrier with the addition of an MFC G2 coating is more than one order of magnitude
 329 compared to what has been found for neat PLA. Moreover, the adhesion between two layers was

330 still stable as the bilayer film performed well within the temperature range investigated under dry
331 oxygen permeation measurements.

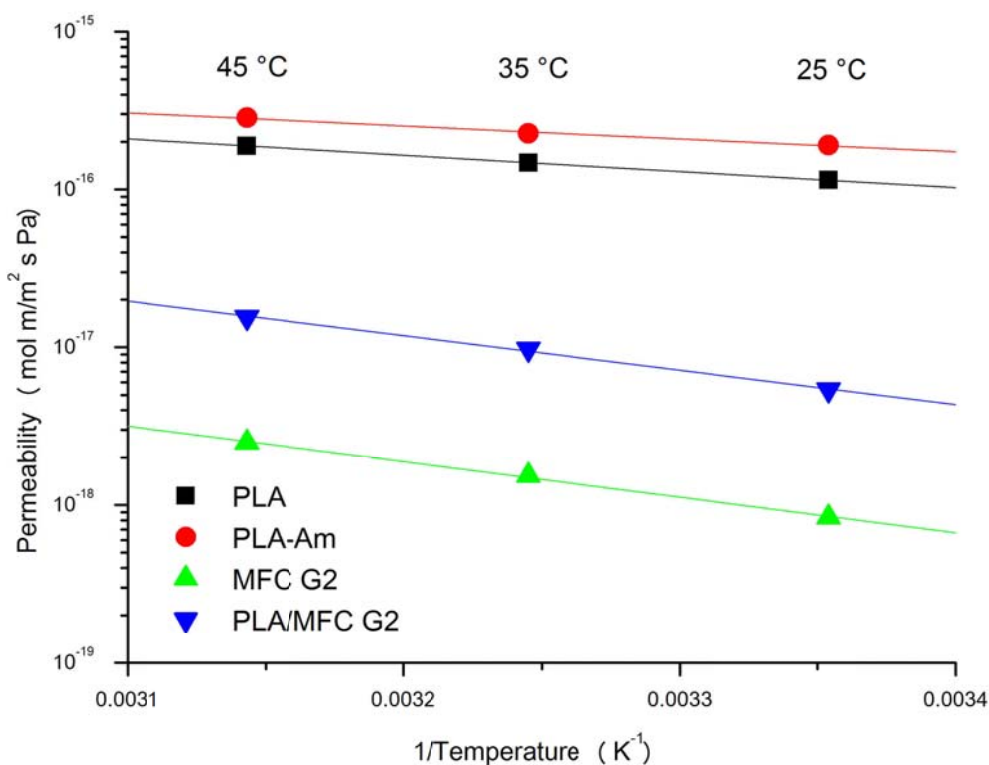
332 Interestingly, the O₂ permeability in MFC films increases significantly at increasing
333 temperature, appreciably more than in pure PLA films, following an Arrhenius relationship:

$$334 \quad P = P_0 \cdot \exp\left(-\frac{E_p}{RT}\right) \quad (2)$$

335 This indicates a larger activation energy of the gas transport process for MFC films, and
336 consequently for PLA/MFC multilayer systems. The calculated values of activation energy of
337 permeation are 19.6 and 15.7 kJ/mol for amorphous and semicrystalline PLA, respectively, while
338 the value of 41.8 kJ/mol is obtained for MFC self-standing films.

339 The barrier performances of the bilayer film were also evaluated in humid conditions,
340 relevant in the packaging sector, and in view of the very hydrophilic nature of cellulosic
341 materials. As already mentioned, the MFC coatings are firmly attached to the PLA substrates and
342 no delamination is observed even in highly humid environments. Oxygen permeability at various
343 humidity contents was then measured in PLA/MFC G1 and PLA/MFC G2 films, and successive
344 experiments at increasing and decreasing trends of R.H. were carried out in order to investigate if
345 any structural changes are induced in the multilayer materials, which might reduce the barrier
346 ability. Fig. 5 shows the oxygen permeability obtained behavior at 35 °C in PLA/MFC G1 and
347 PLA/MFC G2 films with respect to water activity (R.H.).

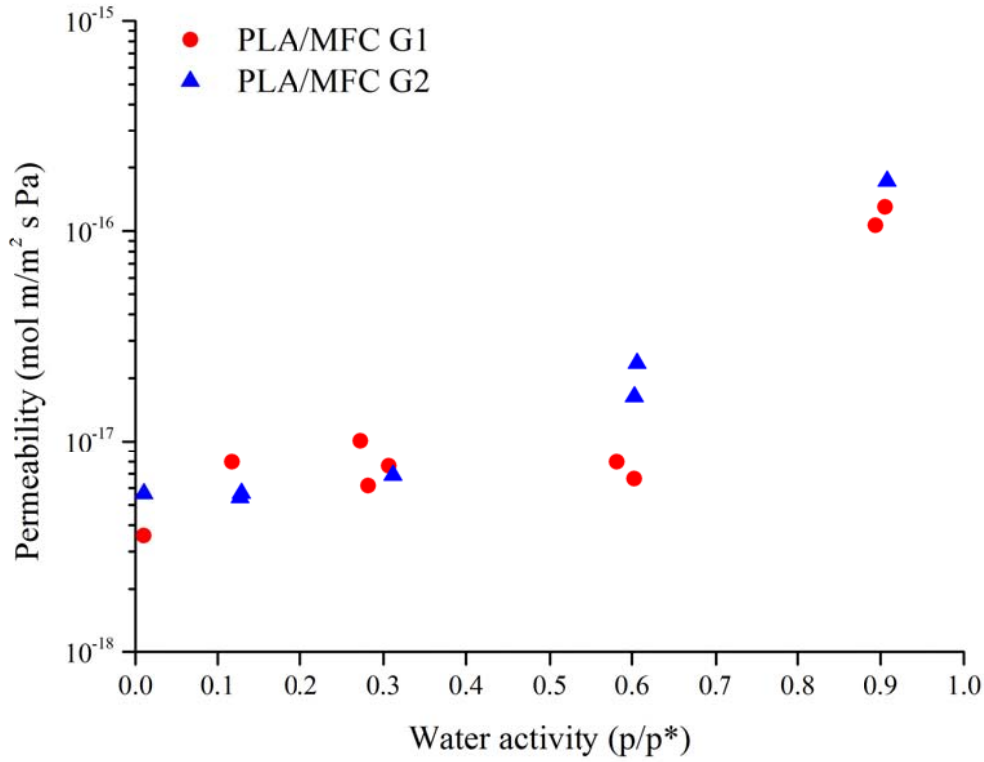
348



349

350 **Fig. 4.** Oxygen permeability of PLA films (semi-crystalline or amorphous) as self-
 351 standing MFC or PLA/MFC G2 multilayer films at different temperatures (25-45 °C), in dry
 352 conditions (R.H. = 0).
 353

354 The values reported in the figure represent effective values of permeability of the bilayer
 355 materials, as they are obtained dividing the OTR for the total coating thickness. As one can see,
 356 the addition of a thin MFC layer produced remarkable enhancement of the barrier effect, which
 357 is preserved up to 60% of R.H.. The sharp raise of permeability at higher water activities (for
 358 both MFC G1 and MFC G2) is mainly due to the large water sorption in the MFC layer and the
 359 consequent swelling, which loosened of the original barrier properties. The ultimate oxygen
 360 permeability at 90% R.H. reached the value of pure PLA, indicating that, in such conditions,
 361 there is no more barrier effect provided by the MFC coating.



362

363 **Fig. 5.** Humid oxygen permeation for PLA/MFC G1 and PLA/MFC G2 films at 35 °C

364

365 It is noteworthy that data in Figure 4 has been retrieved in many successive cycles of R.H.

366 increasing and decreasing ramps, and the bilayer films demonstrated to withstand different

367 humidity conditions without showing any aging in terms of barrier properties or loss of adhesion.

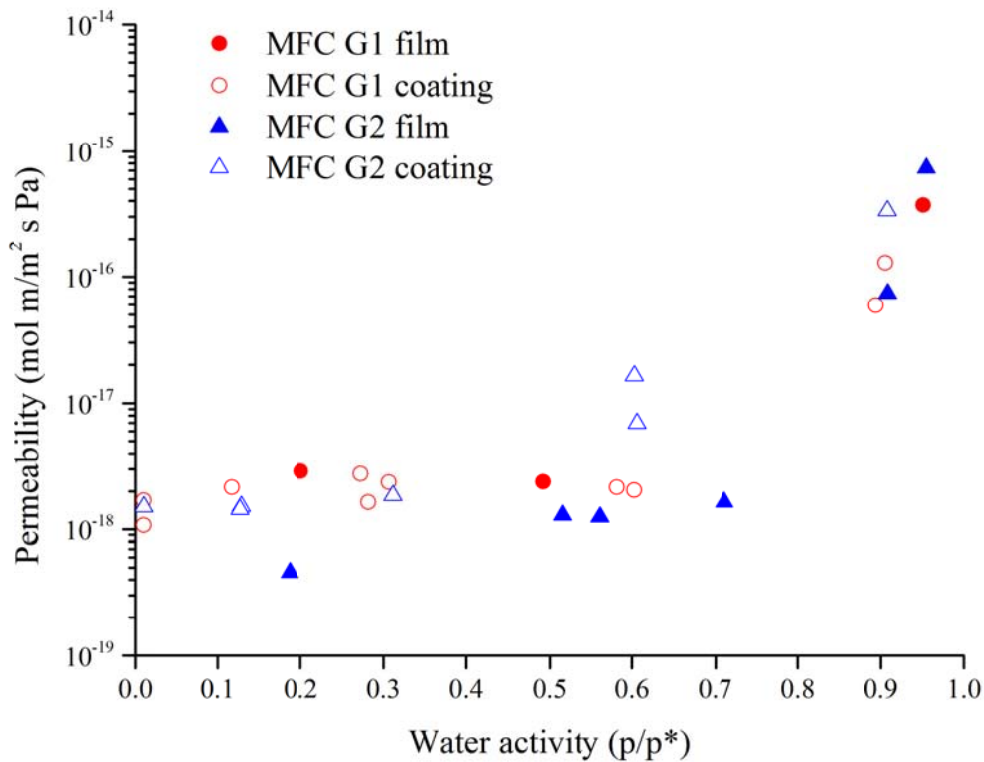
368 Based on the OTR data of the bilayer system, and the knowledge of PLA permeability the sole

369 performance of the coating layer of MFC can be evaluated by means of series resistance formula:

370
$$\frac{1}{(OTR)_{ML}} = \frac{1}{(OTR)_{PLA}} + \frac{1}{(OTR)_{MFC}} = \frac{\delta_{PLA}}{P_{PLA}} + \frac{\delta_{MFC}}{P_{MFC}} \quad (3)$$

371
$$P_{MFC} = \delta_{MFC} \left[\frac{1}{(OTR)_{ML}} - \frac{\delta_{PLA}}{P_{PLA}} \right]^{-1} \quad (4)$$

372 Fig. 6 compares the oxygen permeability of self-standing MFC films measured at 35 °C to those
373 of the coating layer in the bilayer film, as determined by Eq. 3, in order to analyze the coating
374 performances. As one can see, the behavior of MFC coatings is quite similar to that in the self-
375 standing films and only small differences are visible, indicating that a dense and homogeneous
376 coating layer has been obtained with no apparent defect, in agreement with what already
377 suggested by mechanical tests and SEM images.



378

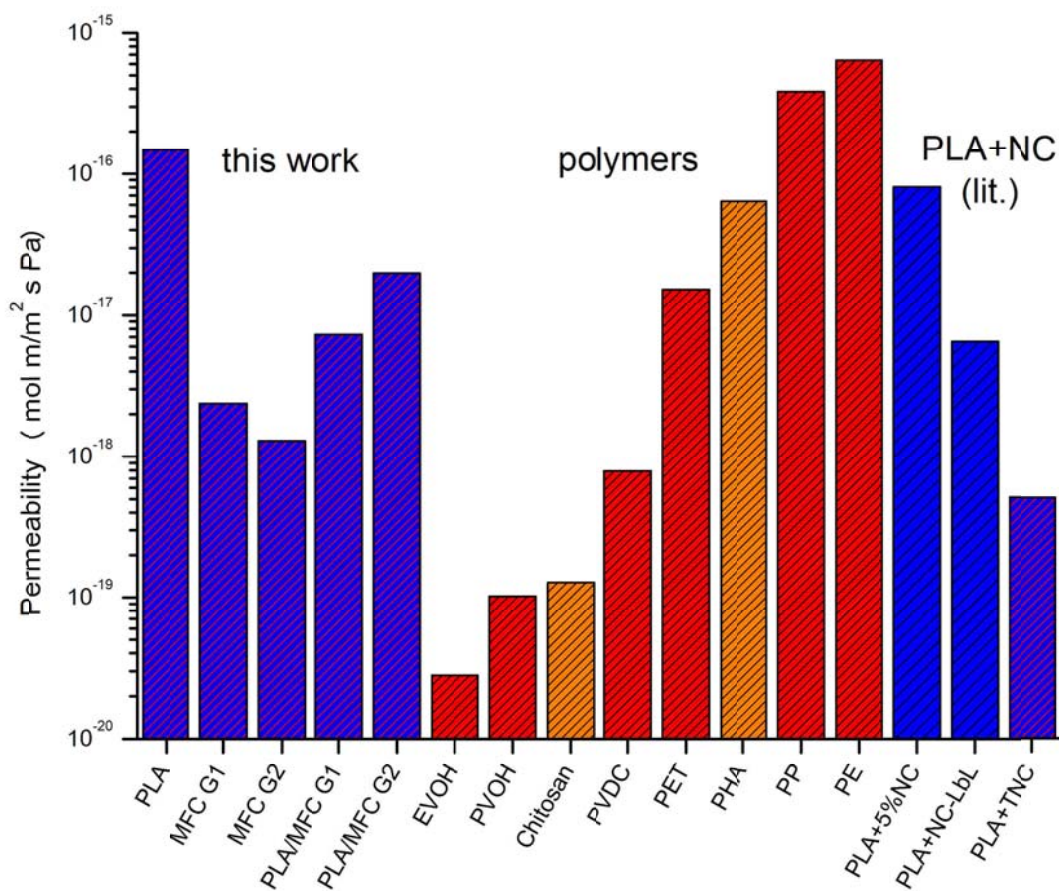
379 **Fig. 6.** Comparison of oxygen permeability for neat MFC film and MFC coating layer

380

381 Finally, the experimental permeability data at 35 °C at 50% R.H. of the samples analyzed
382 in this work are summarized in Fig. 7, which compares their barrier performance with those of
383 conventional oil-based polymers and other bio-renewable materials, all relevant in the packaging
384 sector, as well as with some PLA/nanocellulose composite systems. Data from the literature are

385 obtained at 23 °C and 50% R.H. (Butler et al., 1996; van Tuil et al. 2000; Lange and Wyser,
 386 2003; Aulin et al., 2013; Fortunati et al., 2012; Fukuzumi et al., 2013); however as one can see,
 387 PLA/MFC bilayer films are able to provide, even at higher temperature and in a humid
 388 environment (50% R.H.), a remarkable barrier effect toward oxygen, comparable or better to
 389 most of the conventional and renewable polymer materials.

390



391

392 **Fig. 7.** Comparison of the oxygen permeabilities at (50% RH) obtained on the samples prepared
 393 in this work, with those of common polymers. (Butler et al., 1996; van Tuil et al. 2000; Lange
 394 and Wyser, 2003; Aulin et al., 2013; Fortunati et al., 2012; Fukuzumi et al., 2013)

395

396 **4. Conclusions**

397 In the present study, a fully biodegradable and biorenewable multilayer film has been
398 developed coupling, by means of an environmental friendly method needing no additional
399 chemicals, two primarily incompatible polymeric materials. A MFC coating was indeed
400 deposited onto a plasma activated PLA substrate, aiming at the fabrication of an oxygen barrier
401 and water resistant solution for barrier packaging applications. The atmospheric plasma surface
402 activation of the PLA substrate promoted a strong adhesion between two layers, as observed by
403 SEM micrographs and by mechanical analysis, which revealed an improved behavior of the PLA
404 film in presence of the MFC coating.

405 The plasma assisted methodology, indeed, offers a sustainable tool for the fabrication of
406 effective and stable barrier coatings on biopolymer substrates, and the presented DBD-roller
407 plasma source has the potential for the scale up and the integration in “in-line” procedures for
408 industrial production of multilayer films.

409 The oxygen permeability of bilayer films in dry conditions showed a remarkable barrier
410 effect produced by the addition of the MFC coating on PLA substrate. As a decrease of the
411 O.T.R. of about one order of magnitude was indeed observed that interestingly was preserved
412 also in humid environments (up to about 60% RH at least), as revealed by the investigation of the
413 gas permeability at various water activities. The oxygen permeability of present materials then
414 resulted to be much lower than most of the conventional oil-based and novel bio-based barrier
415 solutions at 50% R.H.

416 The calculation of the coating permeability (from series resistance expression) and its
417 comparison with pure MFC permeability data revealed very similar results for MFC coating or
418 self-standing films, confirming the a dense and stable thin top layer is achieved without any
419 cracks or detachment from PLA substrate.

420

421 **ACKNOWLEDGMENTS**

422 The authors gratefully acknowledge financial support provided through the EU Seventh
423 Framework NEWGENPAK project and COST Action FP 1003 BioMatPack for the research
424 reported in this paper.

425

426 **REFERENCES**

- 427 – Andresen, M., Stenstad, P., Møretrø, T., Langsrud, S., Syverud, K., Johansson, L. S., &
428 Stenius, P. (2007). Nonleaching antimicrobial films prepared from surface-modified
429 microfibrillated cellulose. *Biomacromolecules*, 8, 2149–2155.
- 430 – Ansaloni, L., Minelli, M., Giacinti Baschetti, M. Sarti, G. C. (2014) Effect of relative
431 humidity and temperature on gas transport in Matrimid: Experimental study and
432 modeling, *J. Membr. Sci.* 47, 1392–401
- 433 – ASTM Standard D 1434, 1982 (2009), "Test method for determining gas permeability
434 characteristics of plastic film and sheeting" ASTM International, West Conshohocken,
435 PA, **2009**, DOI: 10.1520/D1434-82R09E01, www.astm.org.
- 436 – Aulin, C., Karabulut, E., Tran, A., Wågberg, L., Lindström, T. (2013) Transparent
437 nanocellulosic multilayer thin films on polylactic acid with tunable gas barrier properties,
438 *ACS Appl. Mater. Interfaces* 5, 7352–7359.
- 439 – Auras, R. A., Harte, B., Selke, S., Hernandez, R. J. (2003). Mechanical, physical, and
440 barrier properties of poly (lactide) films, *J. Plastic Film Sheet.*, 19, 123–135.
- 441 – Auras, R., Kale, G., Singh, S. P. (2006). Degradation of commercial biodegradable
442 packages under real composting and ambient exposure conditions, *J. Environ. Polym.*
443 *Degr.* 14, 317–334.
- 444 – Bai, H., Huang, C., Xiu, H., Zhang, Q., Deng, H., Wang, K., Chen, F., Fu Q. (2014)
445 Significantly improving oxygen barrier properties of polylactide via constructing parallel-
446 aligned shish-kebab-like crystals with well-interlocked boundaries. *Biomacromolecules*
447 15, 1507-1514.
- 448 – Bardet, R., Reverdy, C., Belgacem, N., Leirset, I., Syverud, K., Bardet, M., Bras, J.
449 (2015) Substitution of nanoclay in high gas barrier films of cellulose nanofibrils with
450 cellulose nanocrystals and thermal treatment, *Cellulose* 22, 1227–1241
- 451 – Belbekhouche, S., Bras, J., Siqueira, G., Chappey, C., Lebrun, L., Khelifi, B., Marais, S.,
452 Dufresne, A. (2011). Water sorption behavior and gas barrier properties of cellulose
453 whiskers and microfibrils films. *Carbohydr. Polym.* 83, 1740-1748.
- 454 – Benetto E., Jury C., Igos E., Carton J., Hild P., Vergne C., Di Martino J. (2015). Using
455 atmospheric plasma to design multilayer film from polylactic acid and thermoplastic
456 starch: a screening Life Cycle Assessment, *J. Clean Prod.* 87, 953.
- 457 – Berglund, L., (2005). Cellulose-based nanocomposites, in *Natural Fibres, Biopolymers*
458 *and Biocomposites*, ed. A. K. Mohanty, M. Misra and L. T. Drzal, Taylor & Francis,
459 Boca Raton, pp. 807–832.

- 460 – Boselli, M., Colombo, V., De Angelis, M. G., Ghedini, E., Gherardi, M., Laurita, R.,
461 Liguori, A., Minelli M., Sanibondi, P., Stancampiano, A. (2012). Comparing the effect of
462 different atmospheric pressure non-equilibrium plasma sources on PLA oxygen
463 permeability, *J. Phys. Conf. Ser.*, 406, 012038.
- 464 – Boselli, M., Colombo, V., Ghedini, E., Gherardi, M., Laurita, R., Liguori, A., Marani, F.,
465 Sanibondi, P., & Stancampiano, A. (2013). Parametric study on the effectiveness of
466 treatment of polyethylene (pe) foils for pharmaceutical packaging with a large area
467 atmospheric pressure plasma source. 2013 (August); proceedings of 21st International
468 Symposium on Plasma Chemistry", Queensland (Australia); 495 PO.
- 469 – Butler, B. L., Vergano, P. J., Testin, R. F., Bunn, J. M., Wiles, J. L., (1996) Mechanical
470 and barrier properties of edible chitosan films as affected by composition and storage. *J.*
471 *Food Sci.*, 61, 953.
- 472 – Chang, J. H., An, Y. U., Sur, G. S. J. (2003). Poly(lactic acid) nanocomposites with
473 various organoclays. I. Thermomechanical properties, morphology, and gas permeability,
474 *J. Polym. Sci.: Polym. Phys.*, 41, 94–103.
- 475 – Chowdhury, S. R. (2008). Some important aspects in designing high molecular weight
476 poly(L-lactic acid)–clay nanocomposites with desired properties, *Polym. Int.*, 57,
477 1326–1332.
- 478 – Cools P., De Geyter N., Morent R., (2015). PLA enhanced via plasma technology: a
479 review, *New Developments in Polylactic Acid Research*, Nova Science Publishers, Inc.,
480 Courtney Winthrop pp. 79-110.
- 481 – de Azeredo, H. M. C. (2009) Nanocomposites for food packaging applications, *Food Res.*
482 *Int.*, 42, 1240–1253.
- 483 – Delpouve, N., Stoclet, G., Saiter, A., Dargent, E., Marais, S. (2012) Water barrier
484 properties in biaxially drawn poly(lactic acid) films, *J. Phys. Chem. B* 116, 4615–4625.
- 485 – Drieskens, M., Peeters, R., Mullens, J., Franco, D., Lemstra, P. J., Hristova-Bogaerds, D.
486 G. (2009). Structure versus properties relationship of poly(lactic acid). I. Effect of
487 crystallinity on barrier properties, *J. Polym. Sci., Part B: Polym. Phys.*, 47, 2247–2258.
- 488 – Drumright, R. E., Gruber, P. R., Henton, D. E. (2000). Polylactic acid technology, *Adv.*
489 *Mater.* 12, 1841–1846.
- 490 – Eichhorn S.J., (2011). Cellulose nanowhiskers: promising materials for advanced
491 applications, *Soft Matter*, 7, 303-315.
- 492 – Fortunati, E., Peltzer, M., Armentano, I., Torre, L. Jiménez, A., Kenny, J. M. (2012)
493 Effects of modified cellulose nanocrystals on the barrier and migration properties of PLA
494 nano-biocomposites, *Carbohydr. Polym.* 90, 948– 956.

- 495 – Fukuzumi, H., Saito, T., Wata, T., Kumamoto, Y., Isogai, A. (2009). Transparent and
496 High Gas Barrier Films of Cellulose Nanofibers Prepared by TEMPO-Mediated
497 Oxidation Biomacromolecules, 10, 162–165.
- 498 – Fukuzumi, H., Saito, T., Kumamoto, Y., Isogai, A. (2013). Influence of TEMPO-
499 oxidized cellulose nanofibril length on film properties, Carbohydr. Polym, 93, 172– 177.
- 500 – Guinault A., Sollogoub, C., Ducruet, V., Domenek, S. (2012) Impact of crystallinity of
501 poly(lactide) on helium and oxygen barrier properties, Eur. Polym. J. 48, 779–788.
- 502 – Habibi, Y. (2014) Key advances in the chemical modification of nanocelluloses, Chem.
503 Soc. Rev. 43, 1519-1542.
- 504 – Henriksson, M., Berglund, L. A., (2007). Structure and properties of cellulose
505 nanocomposite films containing melamine formaldehyde, J. Appl. Polym. Sci., 106,
506 2817.
- 507 – Henriksson, M., Henriksson. G., Berglund, L. A., Lindstrom, T. (2007) An
508 environmentally friendly method for enzyme-assisted preparation of microfibrillated
509 cellulose (MFC) nanofibers, Eur. Polym. J. 43, 3434–3441
- 510 – Henriksson, M., Berglund, L. A., Isaksson, P., Lindström, T., Nishino, T. (2008).
511 Cellulose nanopaper structures of high toughness. Biomacromolecules, 9, 1579–1585.
- 512 – Herrick, F. W., Casebier, R. L., Hamilton, K. J., Sandberg, K. R. (1983). Microfibrillated
513 cellulose: morphology and accessibility. J. Appl. Polym. Sci.: Appl. Polym. Symp. 37,
514 797–813.
- 515 – Iwatake, A., Nogi, M., Yano, H. (2008). Cellulose nanofiber-reinforced polylactic acid,
516 Compos. Sci. Technol., 68, 2103-2106
- 517 – Jamshidian M., Tehrany E. A., Imran M., Jacquot M., Desobry S. (2010) Poly-Lactic
518 Acid: production, applications, nanocomposites, and release studies, Compr. Rev. Food
519 Sci. Food Safety, 9, 552–571
- 520 – Johansson, C., Bras, J., Mondragon, I., Nechita, P., Plackett, D., Šimon, P., Aucejo, S.
521 (2012). Renewable fibers and bio-based materials for packaging applications - A review
522 of recent developments. BioResources. 7, 2506–2552
- 523 – Jordá-Vilaplana A., Fombuena V., García-García D., Samper M.D., Sánchez-Nácher L.,
524 (2014). Surface modification of polylactic acid (PLA) by air atmospheric plasma
525 treatment Eur. Polym. J. 58, 23.
- 526 – Klemm, D., Schumann, D., Kramer, F., Heßler, N., Hornung, M., Schmauder, H.-P., et al.
527 (2006). Nanocelluloses as innovative polymers in research and application. In D. Klemm
528 (Ed.), Polysaccharides II (pp. 49–96). Berlin, Heidelberg: Springer.

- 529 – Lange, J., Wyser, Y. (2003). Recent innovations in barrier technologies for plastic
530 packaging - a review. *Pack. Tech. Sci.*, 16, 149
- 531 – Lavoine, N., Desloges, I., Dufresne, A., Bras, J. (2012). Microfibrillated cellulose – Its
532 barrier properties and applications in cellulosic materials: A review. *Carbohydr. Polym.*
533 90, 735–764.
- 534 – Lavoine, N., Desloges, I., Bras, J. (2014) Microfibrillated cellulose coatings as new
535 release systems for active packaging, *Carbohydr. Polym.* 103, 528–537.
- 536 – Leitner, J., Hinterstoisser, B., Wastyn, M., Keckes, J., Gindl, W. (2007). Sugar beet
537 cellulose nanofibril-reinforced composites. *Cellulose*, 14, 419–425.
- 538 – Lu, J., Askeland, P., & Drzal, L. T. (2008). Surface modification of microfibrillated
539 cellulose for epoxy composite applications. *Polymer*, 49, 1285–1296.
- 540 – Martínez-Sanz, M., Lopez-Rubio, A., Lagaron, J. M. (2013) High-barrier coated bacterial
541 cellulose nanowhiskers films with reduced moisture sensitivity, *Carbohydr. Polym.* 98,
542 1072-1082.
- 543 – Mathew, A. P., Oksman, K., Sain, M. (2005). Mechanical properties of biodegradable
544 composites from poly lactic acid (PLA) and microcrystalline cellulose (MCC), *J. Appl.*
545 *Polym. Sci.*, 97, 2014–2025.
- 546 – Mathew, A. P., Oksman, K., Sain, M. (2006). The effect of morphology and chemical
547 characteristics of cellulose reinforcements on the crystallinity of polylactic acid, *J. Appl.*
548 *Polym. Sci.*, 101, 300–310.
- 549 – Minelli, M., De Angelis, M. G., Doghieri, F., Marini, M., Toselli, M., Pilati, F. (2008).
550 Oxygen permeability of novel organic–inorganic coatings. I. Effects of organic–inorganic
551 ratio and molecular weight of the organic component, *Eur. Polym. J.*, 44, 2581–2588.
- 552 – Minelli, M., Giacinti Baschetti, M., Doghieri, F., Ankerfors, M., Lindström, T., Siró, I.,
553 Plackett, D. (2010). Investigation of mass transport properties of microfibrillated
554 cellulose (MFC) films. *J. Membr. Sci.* 358(1-2), 67–75.
- 555 – Mohanty, A. K., Misra, M., and Drzal, L. T. (2002). Sustainable bio-composites from
556 renewable resources: opportunities and challenges in the green materials World, *J.*
557 *Polym. Environ.* 10, 19-26.
- 558 – Nakagaito, A. N., Fujimura, A., Sakai, T., Hama, Y., Yano, H. (2009). Production of
559 microfibrillated cellulose (MFC)-reinforced polylactic acid (PLA) nanocomposites from
560 sheets obtained by a papermaking-like process. *Compos. Sci. Technol.* 69, 1293.
- 561 – Oksman, K., Mathew, A. P., Bondeson, D., Kvien, I. (2006). Manufacturing process of
562 cellulose whiskers/polylactic acid nanocomposites, *Compos. Sci. Technol.*, 66, 2776–
563 2784.

- 564 – Österberg, M., Vartiainen, J., Lucenius, J., Hippo, U., Seppälä, J., Serimaa, R., Laine, J.
565 (2013). A fast method to produce strong NFC films as a platform for barrier and
566 functional materials. *ACS Appl. Mater. Interfaces* 5, 4640–4647
- 567 – Pääkkö, M., Ankerfors, M., Kosonen, H., Nykänen, A., Ahola, S., Österberg, M.,
568 Lindström, T. (2007). Enzymatic hydrolysis combined with mechanical shearing and
569 high-pressure homogenization for nanoscale cellulose fibrils and strong gels.
570 *Biomacromolecules*, 8, 1934–1941.
- 571 – Petersen, K., Nielsen, P. V., Bertelsen, G. Lawther, M., Olsen, M. B., Nilsson, N. H.,
572 Mortensen, G. (1999). Potential of biobased materials for food packaging, *Trends Food*
573 *Sci. Technol.* 10, 52-68.
- 574 – Picard, E., Espuche, E., Fulchiron, R. (2011). Effect of an organo-modified
575 montmorillonite on PLA crystallization and gas barrier properties, *Appl. Clay Sci.* 53,
576 58–65.
- 577 – Plackett, D., Anturi, H., Hedenqvist, M., Ankerfors, M., Gällstedt, M., Lindström, T.,
578 Siró, I. (2010). Physical properties and morphology of films prepared from
579 microfibrillated cellulose and microfibrillated cellulose in combination with amylopectin.
580 *J. Appl. Polym. Sci.* 117, 3601–3609.
- 581 – *Plastics – the Facts 2015*, An analysis of European plastics production, demand and waste
582 data, *Plastics Europe*.
- 583 – Renouf-Glauser, A. C., Rose, J., Farrar, D. F., Cameron, R. E. (2005) The effect of
584 crystallinity on the deformation mechanism and bulk mechanical properties of PLLA,
585 *Biomaterials* 26, 5771–5782.
- 586 – Rodionova, G., Saito, T., Lenes, M., Eriksen, Ø., Gregersen, Ø., Fukuzumi, H., Isogai A.
587 (2012) Mechanical and oxygen barrier properties of films prepared from fibrillated
588 dispersions of TEMPO-oxidized Norway spruce and Eucalyptus pulps, *Cellulose* 19,
589 705–711.
- 590 – Samir, M.A.S.A, Alloin, F., Dufresne, A. (2005). Review of recent research into
591 cellulosic whiskers, their properties and their application in nanocomposite field.
592 *Biomacromolecules*, 6, 612–626.
- 593 – Sanchez-Garcia, M. D., Lagaron, J. M. (2010). On the use of plant cellulose
594 nanowhiskers to enhance the barrier properties of polylactic acid, *Cellulose*, 17 (5), 987–
595 1004.
- 596 – Siqueira, G., Bras, J., Dufresne, A. (2009). Cellulose whiskers versus microfibrils:
597 influence of the nature of the nanoparticle and its surface functionalization on the thermal
598 and mechanical properties of nanocomposites. *Biomacromolecules*, 10, 425–32.

- 599 – Siracusa V., Rocculi P., Romani S., Dalla Rosa M., (2008) Biodegradable polymers for
600 food packaging: a review, *Trends Food Sci. Technol.*, 19, 634–643
- 601 – Siró, I., Plackett, D. (2010). Microfibrillated cellulose and new nanocomposite materials:
602 A review. *Cellulose*, 17, 459–494.
- 603 – Siró, I., Plackett, D. Hedenqvist, M., Ankerfors, M., Lindstrom, T. (2011) Highly
604 transparent films from carboxymethylated microfibrillated cellulose: the effect of
605 multiple homogenization steps on key properties, *J. Appl. Polym. Sci.* 119, 2652–2660.
- 606 – Stenstad, P., Andresen, M., Tanem, B. S., Stenius, P. (2008). Chemical surface
607 modifications of microfibrillated cellulose. *Cellulose*, 15, 35–45.
- 608 – Suryanegara, L., Nakagaito, A. N., Yano, H. (2009). The effect of crystallization of PLA
609 on the thermal and mechanical properties of microfibrillated cellulose-reinforced PLA
610 composites. *Compos. Sci. Technol.*, 69, 1187.
- 611 – Svagan, A. J., Samir, M.A.S.A., Berglund, L. A. (2007). Biomimetic polysaccharide
612 nanocomposites of high cellulose content and high toughness. *Biomacromolecules*, 8,
613 2556–2563.
- 614 – Svagan A. J., Åkesson, A., Cárdenas, M., Bulut, S., Knudsen, J. C., Risbo, J., Plackett,
615 D., (2012). Transparent films based on PLA and montmorillonite with tunable oxygen
616 barrier properties, *Biomacromolecules*, 13, 397–405.
- 617 – Syverud, K., Stenius, P. (2009). Strength and barrier properties of MFC films. *Cellulose*,
618 16, 75–85.
- 619 – Tharanathan R. N. (2003) Biodegradable films and composite coatings: past, present and
620 future. *Trends Food Sci Technol*, 14, 71–8.
- 621 – Turbak, A. F., Snyder, F. W., Sandberg, K. R. (1983). Microfibrillated cellulose, a new
622 cellulose product: Properties, uses, and commercial potential. *Journal of Applied Polymer
623 Science: Applied Polymer Symposium*, 37, 815–827.
- 624 – van Tuil, R., Fowler, P., Lawther, M., Weber, C.J. (2000). Properties of biobased
625 packaging materials, In Weber, C. J., (ed.), *Biobased Packaging Material for the Food
626 Industry - Status and Perspectives*, Royal Veterinary and Agricultural University,
627 Copenhagen, Denmark, 13-44.
- 628 – Vergne C., Buchheit O., Eddoumy F., Sorrenti E., Di Martino J., Ruch D., (2011).
629 Modifications of the polylactic acid surface properties by dbd plasma treatment at
630 Atmospheric Pressure, *J. Eng. Mater. Technol.* 133, 030903.
- 631 – Vieira M. G. A., da Silva M. A., dos Santos L. O., Beppu M. M., (2011) Natural-based
632 plasticizers and biopolymer films: A review, *Europ. Polym. J.*, 47, Pages 254–263

- 633 – Wågberg, L., Decher, G., Norgren, M., Lindström, T., Ankerfors, M., Axnäs, K. (2008).
634 The build-up of polyelectrolyte multilayers of microfibrillated cellulose and cationic
635 polyelectrolytes. *Langmuir* 24, 784–795.
- 636 – Yano, H.; Nakahara S., (2004). Bio-composites produced from plant microfiber bundles
637 with a nanometer unit web-like network. *J. Mater. Sci.*, 39, 1635–1638.
- 638 – Zimmermann, T., Pöhler, E., Geiger, T. (2004). Cellulose fibrils for polymer
639 reinforcement. *Adv. Eng. Mater.* 6, 754–761.